Synthesis, Structure, and Electrochemistry of Platinum(II) Metallacyclobutanes

R. J. Klingler, J. C. Huffman, and J. K. Kochi*

Contribution from the Department of Chemistry, Indiana University, Bloomington, Indiana 47405. *Received July 20, 1981*

Abstract: The novel platinacyclobutane $\overline{CH_2CH_2CH_2}Pt(bpy)$ (I) is synthesized by either the cathodic or the chemical reduction of the readily available platinum(IV) analogue $\overline{CH_2CH_2CH_2}Pt(bpy)Cl_2$. X-ray crystallography reveals the essential identity of the platinacyclobutane moiety in both the platinum(II) and platinum(IV) derivatives. Unlike the platinum(IV) metallacyclobutane, however, the platinacycle I readily undergoes the replacement of α,α'-bipyridine (bpy) by various monodentate ligands such as *tert*-butyl isocyanide and phosphines, and insertion into the Pt–C bond by sulfur dioxide and carbon monoxide, to afford a series of new organoplatinum(II) complexes. The oxidation and reduction of the various platinum(II) metallacyclobutanes and their derivatives are explored with cyclic voltammetric techniques. The ESR spectra of the paramagnetic platinum(I) anions derived from the cathodic and chemical reduction of the platinacyclobutane I and its derivatives are reported.

Interest in organometallic metallacycles derives from their role as possible key intermediates in a variety of catalytic reactions of organic substrates.[1-9] Metallacyclobutanes have drawn special attention, and many transition-metal derivatives of varying stabilities are now known.[10-14] Of these, the largest number are included among the stable, 6-coordinate platinum(IV) analogues which are readily prepared by the oxidative addition of cyclopropanes to platinum(II) derivatives, e.g.,

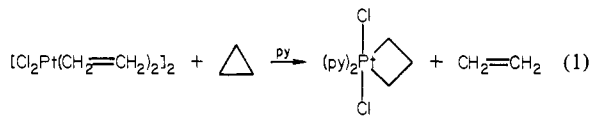

(1)

An excellent review of this subject by Puddephatt has recently appeared.[15] There are fewer examples of the square-planar platinum(II) metallacyclobutanes, which by virtue of their coordinative unsaturation potentially offer greater reactivity than their platinum(IV) counterparts. Although oxidative addition of cyclopropane to platinum(0) complexes is a desirable route to the synthesis of platinum(II) metallacyclobutane, it is presently restricted to cyclopropanes carrying electronegative substituents such as cyano, carbalkoxy, e.g.,[16-18]

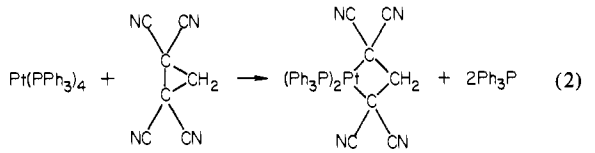

(2)

Foley and Whitesides[19] have prepared the first platinum(II) derivative with a purely hydrocarbon annulus by the thermolysis of dineopentylbis(triethylphosphine)platinum(II) at 157 °C in cyclohexane.

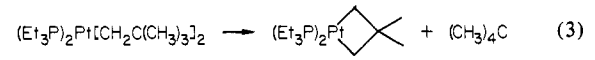

(3)

In this study,[20] we report the synthesis of platinum(II) metallacyclobutanes by the facile reduction of the readily accessible platinum(IV) analogues mentioned above. Moreover, the general electrochemical as well as chemical techniques employed for these platinacyclobutanes can be easily extended to the synthesis of a wide variety of other organometallic systems.

Results

The electrochemical behavior of platinum(IV) metallacyclobutanes[21] is initially explored by cyclic voltammetry (CV). After the cathodic and chemical synthesis of the platinacyclobutane $(bpy)\overline{PtCH_2CH_2CH_2}$, I, its molecular structure was determined by X-ray crystallography, together with that of the platinum(IV) analogue $Cl_2(bpy)\overline{PtCH_2CH_2CH_2}$. The reactivity of the platinacycle I toward various ligands allows two classes of derivatives to be easily prepared—those in which α,α'-bipyridine is replaced by *tert*-butyl isocyanide as well as monodentate phosphines and those in which insertion into the Pt–C bond occurs with carbon monoxide and sulfur dioxide. The unusual ^1H NMR spectra and the oxidation–reduction of the various platinum(II) derivatives are also examined below.

I. Cyclic Voltammetry of Platinum(IV) Metallacycles. The reduction of the platinum(IV) metallacyclobutane $Cl_2(bpy)\overline{PtCH_2CH_2CH_2}$[22] is shown by the cyclic voltammogram in Figure 1, in which two waves are clearly discernible. The first, irreversible cathodic wave occurs in acetonitrile at the peak potential $E_p = -1.35$ V vs. NaCl SCE. Although it shows a well-defined current

(1) For example, see: Grubbs, R. H. *Prog. Inorg. Chem.* **1979**, *24*, 1.
(2) Ivin, K. J.; Rooney, J. J.; Stewart, C. D.; Green, M. L. H.; Mahtab, R. *J. Chem. Soc., Chem. Commun.* **1978**, 604. Green, M. L. H. *Pure Appl. Chem.* **1978**, *50*, 27.
(3) McKinney, R. J. *J. Chem. Soc., Chem. Commun.* **1980**, 490. McKinney, R. J.; Thorn, D. L.; Hoffmann, R.; Stockis, A. *J. Am. Chem. Soc.* **1981**, *103*, 2595.
(4) Fellmann, J. D.; Rupprecht, G. A.; Schrock, R. R. *J. Am. Chem. Soc.* **1979**, *101*, 5099.
(5) Sinfelt, J. H. *Science (Washington D.C.)* **1977**, *195*, 642. Compare also Whitesides (Whitesides, G. M. *Pure Appl. Chem.* **1981**, *53*, 287) for leading references.
(6) Curtis, M. D.; Greene, J. *J. Am. Chem. Soc.* **1978**, *100*, 6362.
(7) (a) Salomon, R. G. *Adv. Chem. Ser.* **1978**, No. *168*, 174. (b) Sarel, S. *Acc. Chem. Res.* **1978**, *11*, 204.
(8) Lenarda, M.; Pahor, N. B.; Calligaris, M.; Graziani, M.; Randaccio, L. *J. Chem. Soc., Dalton Trans.* **1978**, 279.
(9) Sharpless, K. B.; Teranishi, A. Y.; Bäckvall, J. E. *J. Am. Chem. Soc.* **1977**, *99*, 3120. Rappé, A. K.; Goddard, W. A. *Ibid.* **1980**, *102*, 5114.
(10) Moriarty, R. M.; Chen, K.; Yeh, C.; Flippen, J. L.; Karle, T. *J. Am. Chem. Soc.* **1972**, *94*, 8944. Flippen, J. L. *Inorg. Chem.* **1974**, *13*, 1054.
(11) Ephritikhine, M.; Francis, B. R.; Green, M. L. H. *J. Chem. Soc., Dalton Trans.* **1977**, 1131. Adam, G. J. A.; Davies, S. G.; Ford, K. A.; Ephritikhine, M.; Todd, P. F.; Green, M. L. H. *J. Mol. Catal.* **1980**, *8*, 15.
(12) Howard, T. R.; Lee, J. B.; Grubbs, R. H. *J. Am. Chem. Soc.* **1980**, *102*, 6876.
(13) Anderson, R. A.; Jones, R. A.; Wilkinson, G. *J. Chem. Soc., Dalton Trans.* **1978**, 446.
(14) Tulip, T. H.; Thorn, D. L. *J. Am. Chem. Soc.* **1981**, *103*, 2448.
(15) Puddephatt, R. J. *Coord. Chem. Rev.* **1980**, *33*, 149.
(16) Graziani, M.; Lenarda, M.; Ros, R.; Belluco, U. *Coord. Chem. Rev.* **1975**, *16*, 35.
(17) Yarrow, D. J.; Ibers, J. A.; Lenarda, M.; Graziani, M. *J. Organomet. Chem.* **1974**, *70*, 133.
(18) Rajaram, J.; Ibers, J. A. *J. Am. Chem. Soc.* **1978**, *100*, 829.
(19) Foley, P.; Whitesides, G. M. *J. Am. Chem. Soc.* **1979**, *101*, 2732.
(20) Preliminary report: Klingler, R. J.; Huffman, J. C.; Kochi, J. K. *J. Organomet. Chem.* **1981**, *206*, C7.
(21) Adams, D. M.; Chatt, J.; Guy, R. G. *Proc. Chem. Soc. London*, **1960**, 179.
(22) Adams, D. M.; Chatt, J.; Guy, R. G.; Sheppard, N. *J. Chem. Soc.* **1961**, *738*.

0002-7863/82/1504-2147$01.25/0

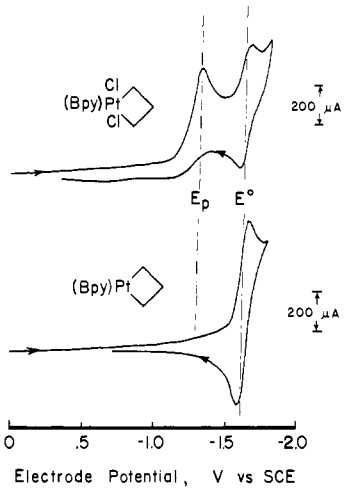

Figure 1. Upper: Initial scan cyclic voltammogram of 1.0×10^{-3} M $Cl_2(bpy)\overline{PtCH_2CH_2CH_2}$ in acetonitrile containing 0.1 M tetraethylammonium perchlorate (TEAP) at a platinum microelectrode with a scan rate of 100 mV s^{-1}. The first irreversible cathodic wave is labeled as E_p. The second reversible wave labeled as E^0 coincides with that of $(bpy)\overline{PtCH_2CH_2CH_2}$ (I) shown in the lower figure.

maximum, no coupled anodic wave is apparent on the reverse scan even at rates up to 10 V s^{-1} and at temperatures as low as −35 °C. The controlled potential electrolysis at −1.35 V requires the passage of 2.03 ± 0.05 electrons per platinum, in accord with the electrochemical reaction in eq 4. Indeed, the platinacyclobutane

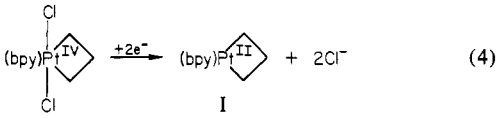

(4)

I was recovered from the electrolyzed solution, and its cyclic voltammogram is characterized by a single reversible wave at E^0 = −1.67 V vs, NaCl SCE, shown in the lower half of Figure 1. Thus the second, reversible wave in the reduction of the platinacyclobutane I corresponds to its further one-electron reduction to the corresponding platinum(I) anion radical, i.e.,

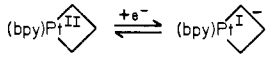

(5)

The cyclic voltammogram of the related 1,10-phenanthroline analogue of platinacyclobutane I, i.e., $Cl_2(4,7\text{-}Ph_2phen)\overline{PtCH_2CH_2CH_2}$, has the same general appearance as that shown in the upper part of Figure 1. (The 4,7-diphenyl-1,10-phenanthroline derivative was used for solubility purposes.) The first irreversible cathodic wave occurs at −1.26 V at a sweep of 200 mV s^{-1}. However, the second couple at E^0 ~−1.58 V is only partially reversible (E_p^c = −1.67 and E_p^a = −1.52 V and i_p^a/i_p^c = 0.5). It is possible that the reductive processes described in eq 4 and 5 for the platinacyclobutane I are partially overlapping in the phenanthroline derivative.

The cyclic voltammogram of the bis(pyridine) analogue of the platinum(IV) metallacyclobutane $Cl_2(py)_2\overline{PtCH_2CH_2CH_2}$[22] shows only a single irreversible cathodic wave at E_p = −1.63 V vs. NaCl SCE. Controlled potential reduction at −1.70 V required 1.87 electrons per platinum. However, the reduction resulted in the complete destruction of the metallacycle moiety, as witnessed by the precipitation of platinum black during the electrolysis, and concomitant liberation of a gaseous mixture (42%) consisting mainly of C_3 fragments, viz., propane (25%), propylene (11%), and cyclopropane (5%).

II. Synthesis and Structural Characterization of the Platinacyclobutane I. The platinacyclobutane I can be isolated as orange crystals in greater than 85% yields from the cathodic reduction of the platinum(IV) metallacyclobutane $Cl_2(bpy)\overline{PtCH_2CH_2CH_2}$ in eq 4. However, it is more conveniently synthesized by the sodium amalgam reduction in acetonitrile at 0 °C, according to the stoichiometry

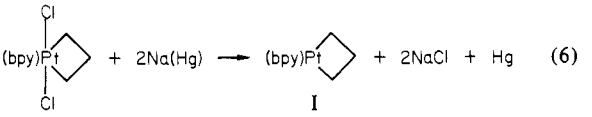

(6)

The orange crystals of the platinacyclobutane I are thermochromic, changing to light yellow upon cooling to −170 °C.

The X-ray diffraction data of I were collected at −170 °C to reduce thermal vibrations and permit the location and refinement of all hydrogens, particularly the six methylene hydrogens. The quality of the diffraction data is reflected in the final discrepancy factors (which were $R(F)$ = 0.036, $R_w(F)$ = 0.037) and a goodness of fit of 1.002 for the last cycle. The molecular structure presented in Figure 2 shows the almost complete planarity of the platinacyclobutane ring.[23] The relevant bond distances and bond angles of only the nonhydrogen atoms are included in Table I. The hydrogen distances and angles are included in the supplementary material (Table XII).

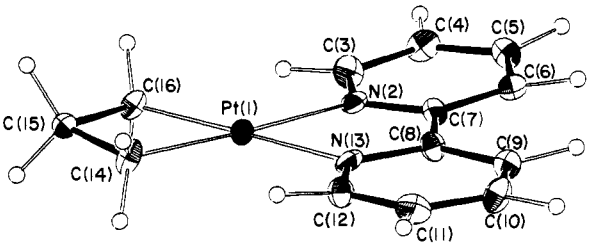

Figure 2. ORTEP drawing of the platinum(II) metallacyclobutane $\overline{CH_2CH_2CH_2}Pt(bpy)$. Anisotropic thermal ellipsoids are drawn at the 50% probability level. Hydrogen atoms are portrayed at 0.5 Å^2.

Table I. Selected Interatomic Distances (Å) and Angles (Deg) in $(bpy)\overline{PtCH_2CH_2CH_2}$ I

A	B	distance	A	B	distance
Pt(1)	N(2)	2.107 (8)	C(4)	C(5)	1.386 (14)
Pt(1)	N(13)	2.103 (4)	C(5)	C(6)	1.377 (14)
Pt(1)	C(14)	2.030 (10)	C(6)	C(7)	1.388 (14)
Pt(1)	C(15)	2.665 (10)	C(7)	C(8)	1.457 (13)
Pt(1)	C(16)	2.037 (10)	C(8)	C(9)	1.383 (13)
N(2)	C(3)	1.348 (13)	C(9)	C(10)	1.400 (15)
N(2)	C(7)	1.349 (13)	C(10)	C(11)	1.365 (15)
N(13)	C(8)	1.381 (12)	C(11)	C(12)	1.376 (14)
N(13)	C(12)	1.314 (12)	C(14)	C(15)	1.534 (14)
C(3)	C(4)	1.368 (15)	C(15)	C(16)	1.534 (13)

A	B	C	angle	A	B	C	angle
N(2)	Pt(1)	N(13)	77.5 (3)	C(4)	C(5)	C(6)	119.2 (9)
N(2)	Pt(1)	C(14)	176.0 (3)	C(5)	C(6)	C(7)	119.4 (10)
N(2)	Pt(1)	C(15)	141.2 (3)	N(2)	C(7)	C(6)	120.8 (9)
N(2)	Pt(1)	C(16)	106.3 (3)	N(2)	C(7)	C(8)	115.2 (9)
N(13)	Pt(1)	C(14)	106.4 (4)	C(6)	C(7)	C(8)	124.1 (9)
N(13)	Pt(1)	C(15)	141.2 (3)	N(13)	C(8)	C(7)	115.9 (8)
N(13)	Pt(1)	C(16)	176.1 (3)	N(13)	C(8)	C(9)	118.8 (9)
C(14)	Pt(1)	C(15)	34.9 (3)	C(7)	C(8)	C(9)	125.3 (9)
C(14)	Pt(1)	C(16)	69.9 (4)	C(8)	C(9)	C(10)	120.4 (9)
C(15)	Pt(1)	C(16)	35.0 (3)	C(9)	C(10)	C(11)	118.7 (10)
Pt(1)	N(2)	C(3)	123.8 (7)	C(10)	C(11)	C(12)	119.0 (10)
Pt(1)	N(2)	C(7)	116.5 (7)	N(13)	C(12)	C(11)	123.1 (10)
C(3)	N(2)	C(7)	119.7 (9)	Pt(1)	C(14)	C(15)	95.8 (6)
Pt(1)	N(13)	C(8)	114.9 (6)	Pt(1)	C(15)	C(14)	49.3 (5)
Pt(1)	N(13)	C(12)	125.1 (7)	Pt(1)	C(15)	C(16)	49.6 (5)
C(8)	N(13)	C(12)	119.9 (8)	C(14)	C(15)	C(16)	98.8 (8)
N(2)	C(3)	C(4)	121.6 (10)	Pt(1)	C(16)	C(15)	95.5 (6)
C(3)	C(4)	C(5)	119.3 (10)				

(23) The flap angle of the β,β-dimethyl analogue in eq 3 has recently been measured as 22°. (Ibers, J. A.; DiCosimo, R.; Whitesides, G. M. *Organometallics* **1981**, *1*, 13.) We thank Professor Ibers for a preprint of this report.

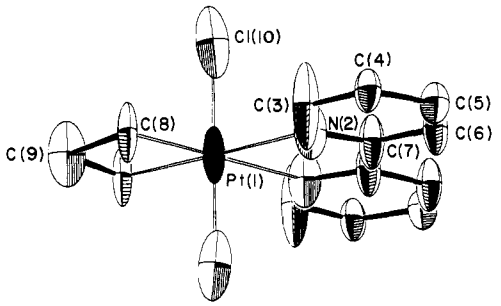

Figure 3. ORTEP drawing of the platinum(IV) metallacyclobutane $\overline{CH_2CH_2CH_2}Pt(bpy)Cl_2$ showing the atomic numbering scheme used in Table II. Thermal ellipsoids are drawn at the 50% probability level.

Table II. Selected Interatomic Distances (Å) and Angles (Deg) in $Cl_2(bpy)\overline{PtCH_2CH_2CH_2}$

A	B	distance	A	B	C	angle
Pt(1)	N(2)	2.20 (3)	N(2)	Pt(1)	N(2)	74.5 (17)
Pt(1)	C(8)	2.07 (4)	N(2)	Pt(1)	C(8)	106.8 (13)
Pt(1)	Cl(10)	2.23 (2)	N(2)	Pt(1)	Cl(10)	90.2 (3)
N(2)	C(3)	1.36 (5)	C(8)	Pt(1)	C(8)	71.9 (23)
N(2)	C(7)	1.30 (5)	C(8)	Pt(1)	Cl(10)	89.8 (3)
C(3)	C(4)	1.41 (5)	Cl(10)	Pt(1)	Cl(10)	179.5 (8)
C(4)	C(5)	1.42 (6)	Pt(1)	N(2)	C(3)	121.5 (31)
C(5)	C(6)	1.36 (6)	Pt(1)	N(2)	C(7)	116.5 (25)
C(6)	C(7)	1.41 (5)	N(2)	C(3)	C(4)	121.1 (41)
C(7)	C(7)	1.51 (8)	C(3)	C(4)	C(5)	117.0 (34)
C(8)	C(9)	1.63 (6)	C(4)	C(5)	C(6)	119.2 (40)
			C(5)	C(6)	C(7)	121.1 (38)
			Pt(1)	C(8)	C(9)	96.0 (30)
			C(8)	C(9)	C(8)	96.2 (51)

III. Crystal Structure Of the Platinum(IV) Metallacyclobutane $Cl_2(bpy)\overline{PtCH_2CH_2CH_2}$. Crystals of the subject platinum(IV) metallacyclobutane suitable for X-ray crystallography were extremely difficult to obtain, owing to problems encountered with the growth of macroscopic crystal twins. After repeated attempts, we were finally able to grow only a small single crystal, which unfortunately limited the precision of the diffraction data and precluded the direct location of the hydrogen atoms. The molecular structure shown in Figure 3 with a planar platinacyclobutane moiety reflects the $2/m$ symmetry required by the diffraction data. The pertinent bond distances and bond angles of the platinum(IV) metallacyclobutane are included in Table II.[24]

IV. Ligand Substitution of the Platinacyclobutane I. The α,α'-bipyridine ligand in $(bpy)\overline{PtCH_2CH_2CH_2}$ is labile and readily displaced by a variety of monodentate ligands described below to afford a series a new platinacyclobutanes $L_2\overline{PtCH_2CH_2CH_2}$ II.

Triphenylphosphine. The addition of triphenylphosphine to an orange solution of $(bpy)\overline{PtCH_2CH_2CH_2}$ in acetonitrile resulted in an immediate lightening of the color, and pale yellow crystals separated over a period of 15 min. Collection of the product, followed by recrystallization from a mixture of ethanol and methylene chloride, yielded colorless needles of the triphenylphosphine derivative IIa. The liberated, free α,α'-bipyridine is also readily removed by sublimation.

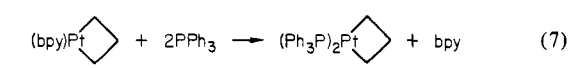

(7)

IIa

Trimethyl- and Triethylphosphine. The orange color of the platinacyclobutane I in acetonitrile was immediately dispelled at 0 °C upon the addition of either trimethyl- or triethylphosphine. The solvent was removed in vacuo and the phosphine adduct either extracted with pentane or the α,α'-bipyridine removed by sublimation in vacuo. Recrystallization from either pentane or hexane afforded colorless crystals of IIb (R = Me) and IIc (R = Et).

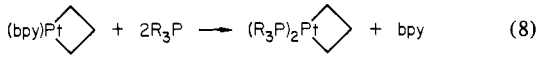

(8)

IIb,c

The latter is directly related to the β,β-dimethyl analogue prepared earlier by Whitesides and co-workers in eq 3.[25]

***tert*-Butyl Isocyanide.** The ligand substitution of $(bpy)\overline{PtCH_2CH_2CH_2}$ with *tert*-butyl isocyanide occurred slowly over a period of 4 h, during which the orange color of the acetonitrile solution gradually lightened only somewhat. After concentration of the orange solution, the pentane extracts afforded white needles of the bis(isocyanide) complex IId. The infrared spectrum of

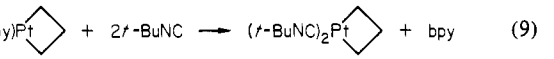

(9)

IId

IId shows two terminal isocyanide bands absorbing at 2160 and 2110 cm^{-1}, characteristic of a cis product.[26-28]

V. Insertion Reactions of the Platinacyclobutanes. Carbon monoxide and sulfur dioxide, which are both commonly used for the study of insertions into a carbon–metal bond,[29] yield isolable adducts with the platinacyclobutanes.

Carbon Monoxide. When a solution of the platinacycle I in acetonitrile was stirred at ambient temperatures under 1 atm of carbon monoxide, it gradually darkened, becoming noticeable only after 15 min. The brown solution after 4 h yielded orange needles of the CO insertion product III, which showed a single, sharp

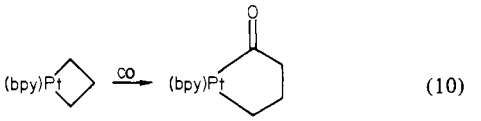

(10)

III

carbonyl band at 1590 cm^{-1} in the infrared spectrum. The structure of the carbonyl adduct was also assigned to III on the basis of the ^1H NMR spectrum showing (a) inequivalent β protons in the coordinated α,α'-bipyridine[32] and (b) the pair of triplets for the two methylene groups, one bonded to platinum (δ 1.41) and the other (δ 2.99) bonded to the carbonyl function. (The central methylene group appears as a multiplet at δ 2.24.)

The continued exposure of an acetonitrile solution of III to an atmosphere of carbon monoxide for prolonged periods (48 h) leads to the dipropionyl complex IV, together with a dark green amorphous solid. The dipropionyl complex was isolated in less

(24) For the crystal structures of the related bis(pyridine) analogues, see: Gillard, R. D.; Keeton, M.; Mason, R.; Pilbrow, M.; Russell, D. R. *J. Organomet. Chem.* **1971**, *33*, 247. McGinnety, J. A. *Ibid.* **1973**, *59*, 429.

(25) Foley, P.; DiCosimo, R.; Whitesides, G. M. *J. Am. Chem. Soc.* **1980**, *102*, 6713.

(26) Cotton, F. A.; Zingales, F. *J. Am. Chem. Soc.* **1961**, *83*, 351.

(27) Badley, E. M.; Chatt, J.; Richards, R. L. *J. Chem. Soc. A* **1971**, 21.

(28) Also see: Wells, P. R. *Prog. Phys. Org. Chem.* **1968**, *6*, 135.

(29) E.g., see: (a) Wojcicki, A. *Adv. Organomet. Chem.* **1973**, *11*, 87. (b) *Ibid.* **1974**, *12*, 31. Kuhlmann, E. J.; Alexander, J. J. *Coord. Chem. Rev.* **1980**, *33*, 195.

(30) (a) See ref 29b. (b) Snow, M. R.; McDonald, J.; Basolo, F.; Ibers, J. A. *J. Am. Chem. Soc.* **1972**, *94*, 2526. Volger, H. C.; Vrieze, K. *J. Organomet. Chem.* **1968**, *13*, 495. Chatt, J.; Mingos, D. M. P. *J. Chem. Soc. A* **1969**, 1770. Graziani, M.; Wojcicki, A. *Inorg. Chim. Acta* **1970**, *4*, 347.

(31) See the tabulations by Puddephatt in ref 15.

(32) The trans influence in the platinacycles included in Table IV is shown in the partially resolved ^1H NMR spectra of the α,α'-bipyridine ligands. Thus in the symmetric platinacycle I, the pyridinyl protons in one ring are equivalent to those in the other, as indicated by resonances at δ 7.44 (2 H), 7.99 (4 H), and 8.92 (2 H). In the carbonyl adduct III, however, one pair of protons [δ 8.94 (1 H) and δ 10.27 (1 H)] is inequivalent as a result of the different trans influence of the carbonyl and methylene moieties. The ligand splittings in the dipropionyl complex IV [δ 7.52 (2 H), 8.02 (4 H), 8.74 (2 H)] are similar to those in I. Compare the bpy resonances in $(bpy)_3M^{3+}$ complexes by: DeSimone, R. E.; Drago, R. S. *J. Am. Chem. Soc.* **1970**, *92*, 2343. La Mar, G. N.; Van Hecke, G. R. *Ibid.* **1969**, *91*, 3442.

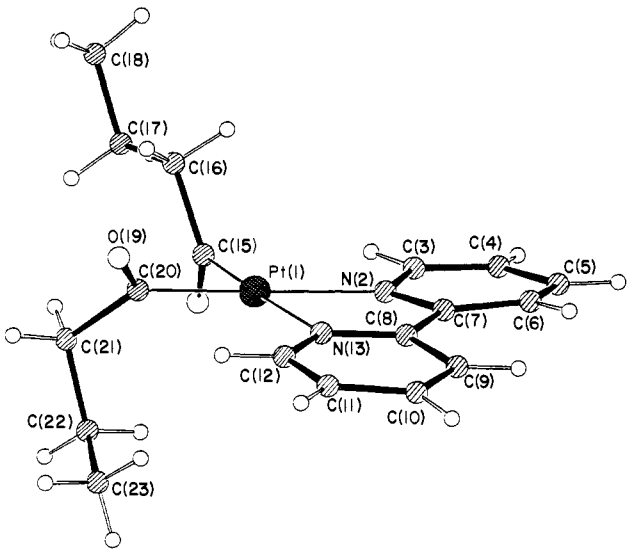

Figure 4. ORTEP drawing of the dipropionylplatinum(II) complex $(CH_3CH_2CH_2CO)_2Pt(bpy)$ (IV) including the atomic numbering scheme used in the tables.

Table III. Selected Interatomic Distances (Å) and Angles (Deg) in $(bpy)Pt(COCH_2CH_2CH_3)_2$, IV

A	B	distance	A	B	distance
Pt(1)	N(2)	2.132 (14)	C(6)	C(7)	1.393 (27)
Pt(1)	N(13)	2.145 (14)	C(7)	C(8)	1.472 (25)
Pt(1)	C(15)	1.969 (18)	C(8)	C(9)	1.409 (25)
Pt(1)	C(20)	2.000 (18)	C(9)	C(10)	1.393 (28)
O(14)	C(15)	1.228 (21)	C(10)	C(11)	1.394 (27)
O(19)	C(20)	1.173 (22)	C(11)	C(12)	1.360 (25)
N(2)	C(3)	1.343 (23)	C(15)	C(16)	1.524 (27)
N(2)	C(7)	1.392 (23)	C(16)	C(17)	1.472 (27)
N(13)	C(8)	1.333 (21)	C(17)	C(18)	1.477 (33)
N(13)	C(12)	1.333 (24)	C(20)	C(21)	1.583 (28)
C(3)	C(4)	1.360 (26)	C(21)	C(22)	1.493 (30)
C(4)	C(5)	1.397 (28)	C(22)	C(23)	1.506 (29)
C(5)	C(6)	1.339 (27)			

A	B	C	angle	A	B	C	angle
N(2)	Pt(1)	N(13)	77.0 (6)	C(6)	C(7)	C(8)	126.7 (18)
N(2)	Pt(1)	C(15)	97.8 (7)	N(13)	C(8)	C(7)	116.5 (15)
N(2)	Pt(1)	C(20)	173.7 (7)	N(13)	C(8)	C(9)	121.7 (16)
N(13)	Pt(1)	C(15)	174.7 (6)	C(7)	C(8)	C(9)	121.6 (17)
N(13)	Pt(1)	C(20)	97.2 (7)	C(8)	C(9)	C(10)	118.3 (17)
C(15)	Pt(1)	C(20)	88.0 (8)	C(9)	C(10)	C(11)	119.0 (18)
Pt(1)	N(2)	C(3)	125.7 (13)	C(10)	C(11)	C(12)	118.1 (18)
Pt(1)	N(2)	C(7)	114.8 (12)	N(13)	C(12)	C(11)	124.3 (18)
C(3)	N(2)	C(7)	119.1 (16)	Pt(1)	C(15)	O(14)	122.9 (15)
Pt(1)	N(13)	C(8)	116.0 (11)	Pt(1)	C(15)	C(16)	119.2 (12)
Pt(1)	N(13)	C(12)	125.4 (13)	O(14)	C(15)	C(16)	117.9 (16)
C(8)	N(13)	C(12)	118.5 (15)	C(15)	C(16)	C(17)	117.0 (17)
N(2)	C(3)	C(4)	122.7 (18)	C(16)	C(17)	C(18)	110.8 (20)
C(3)	C(4)	C(5)	118.7 (18)	Pt(1)	C(20)	O(19)	125.3 (14)
C(4)	C(5)	C(6)	119.1 (18)	Pt(1)	C(20)	C(21)	116.3 (14)
C(5)	C(6)	C(7)	121.9 (20)	O(19)	C(20)	C(21)	118.3 (17)
N(2)	C(7)	C(6)	118.1 (17)	C(20)	C(21)	C(22)	113.8 (18)
N(2)	C(7)	C(8)	115.3 (17)	C(21)	C(22)	C(23)	111.9 (17)

than 50% yields as red needles, showing infrared bands at 1590 and 1620 cm^{-1}. The crystal of IV is thermochromic, changing from dark red at room temperature to pale orange at −170 °C. The X-ray crystal structure of IV is shown in Figure 4, which clearly delineates the pair of *cis*-propionyl ligands. The relevant bond distances and bond angles are included in Table III. The hydrogen distances and angles are in Table XII of the supplementary material.

Attempts to crystallize the dark green byproduct were unsuccessful. However, the infrared spectrum showed two strong, broad carbonyl bands at 1860 and 2050 cm^{-1}. Coupled with the observation of weak but discrete bipyridine resonances in the ^1H NMR spectrum (the presence of bpy was also evident in KBr

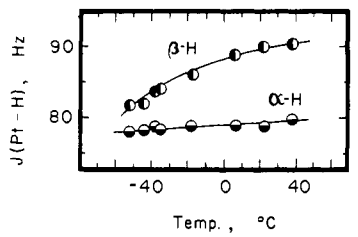

Figure 5. Temperature dependences of the $^{195}Pt-^1H$ coupling constants for the α protons (⊖) and β protons (◐) in the ^1H NMR spectrum of the platinacyclobutane $(bpy)\overline{PtCH_2CH_2CH_2}$ in chloroform solution.

spectrum), we tentatively assign the structure of the green solid to a polymeric dicarbonyl(bipyridine)platinum(0) species, consistent with the (partial) stoichiometry in eq 11.

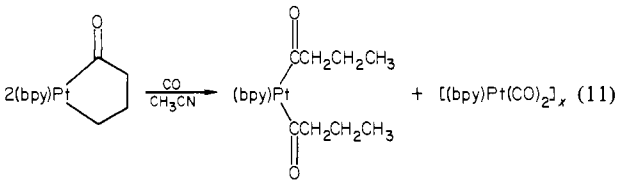

IV

Sulfur Dioxide. Exposure of an acetonitrile solution of the platinacyclobutane I to 1 atm of sulfur dioxide leads to an immediate decoloration of the orange color and precipitation of a yellow solid. Unfortunately, the sulfur dioxide adduct was too insoluble to recrystallize or to work with. However, an infrared spectrum (KBr pellet) showed weak bands at 1080 and 1155 cm^{-1}. Accordingly, we directed our attention to the more soluble platinacyclobutane IIb, i.e., $(Me_3P)_2\overline{PtCH_2CH_2CH_2}$. Indeed, a solution of IIb in pentane also reacted with sulfur dioxide within 5 min to afford a yellow precipitate, which upon recrystallization from acetonitrile at −20 °C yielded white needles of the sulfur dioxide adduct. The infrared spectrum of the sulfur dioxide adduct showed a strong, broad band at 1160 cm^{-1} and a weak band at 1200 cm^{-1}, which we tentatively assign to the symmetric and asymmetric modes, respectively, of the sulfinate-*S* structure V.[30]

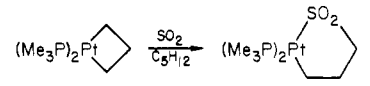

V

VI. ^1H and ^{13}C NMR Spectra of Platinum(II) Metallacyclobutanes and Derivatives. The series of the 16-electron platinacyclobutanes listed in Table IV show rather unusual chemical shifts of the β protons of the $CH_2CH_2CH_2$ moiety in the ^1H NMR spectra. Furthermore, the couplings of the ^{195}Pt and ^{31}P nuclei to the β protons are exceptional, in many cases actually being larger than the corresponding α couplings. By contrast, neither the platinum(IV) analogue $Cl_2L_2\overline{PtCH_2CH_2CH_2}$ nor the related platinum(II) metallacyclopentane $(Ph_3P)_2\overline{PtCH_2CH_2CH_2CH_2}$ exhibits resolved splittings to the β protons.[31] The ^1H NMR spectra of the insertion products are also included in Table VI for comparison.[32]

In the phosphine derivatives IIa–c, the proton–proton couplings in $CH_2CH_2CH_2$ are adequately described as an A_4X_2 system, which results in the observation of a triplet and quintet for the α- and β-methylene protons, respectively, after decoupling the ^{31}P nucleus. The temperature-dependence study of the ^1H NMR spectrum was carried out with IIb, since it was the most soluble platinacyclobutane in chloroform solution down to -50 °C. Over this temperature range, the variation in the proton chemical shift was too small to be measured. However, there are two interesting spectral changes which do accompany the lowering of the temperature. First, the α and β protons show quite distinct differences in the temperature dependences of the $^{195}Pt-^1H$ coupling constants, as illustrated in Figure 5. Second, when the temperature is

Table IV. ^{1}H NMR Spectra of Platinacyclobutanes and Derivatives[a]

platinum complex	coupling constants, Hz $J(^{195}$Pt-H) H_α	$J(^{195}$Pt-H) H_β	$J(^{31}$P-H) H_α	$J(^{31}$P-H) H_β	J $(H_\alpha-H_\beta)$	chemical shifts, δ H_α	H_β	^{31}P	ligand resonances
I, (bpy)PtCH$_2$CH$_2$CH$_2$	115	110			7	1.29 (t)	3.32 (q)		7.44,[d] 7.99,[d] 8.92[d]
IIa, (Ph$_3$P)$_2$PtCH$_2$CH$_2$CH$_2$	88	112	*c*	*c*	*c*	0.37	3.51 (q)	26.104	7.24,[d] 7.50[d]
IIb, (Me$_3$P)$_2$PtCH$_2$CH$_2$CH$_2$	82	95	*c*	*c*	*c*	0.47 (t)	3.74 (m)		1.41[e]
IIc, (Et$_3$P)PtCH$_2$CH$_2$CH$_2$	80	94	5.5	4.3	8	0.35 (t)	3.75 (q)	8.136	1.72,[d] 1.12[d]
IId, (*t*-BuNC)$_2$PtCH$_2$CH$_2$CH$_2$[b]	80	90			8	1.52 (t)	4.58 (q)		0.87[f]
III, (bpy)PtCOCH$_2$CH$_2$CH$_2$	68	104			7	1.41 (t)	2.24 (m) 2.99 (t)[g]		7.56,[d] 8.01,[d] 8.94[d] 10.27[d]
IV, (bpy)Pt(COCH$_2$CH$_2$CH$_3$)$_2$	*c*	*c*			7	2.51 (t)	1.71 (m) 0.86 (t)[h]		7.52,[d] 8.02,[d] 8.74[d]
V, (Me$_3$P)$_2$PtSO$_2$CH$_2$CH$_2$CH$_2$	*c*	*c*	*c*	*c*	8	*c*	2.77 (t)		1.64 (J_{31P} = 8.6)[e] 1.49 (J_{31P} = 9.2)[e]

[a] Spectra measured in $DCCl_3$ except as noted. Coupling constants in Hz. ^{1}H chemical shifts in δ relative to Me_4Si. ^{31}P chemical shifts in ppm relative to external H_3PO_4. [b] C_6D_6. [c] Not resolved. [d] Multiplet. [e] Doublet. [f] Singlet. [g] Methylene bonded to CO. [h] δ proton.

Table V. ^{13}C NMR Spectra of Platinacyclobutanes and Analogues

platinum	chemical shift, δ C_α	C_β	coupling constants, Hz ^{195}Pt-C_α	^{195}Pt-C_β	^{31}P-C_α
(Ph$_3$P)$_2$PtCH$_2$CH$_2$CH$_2$[a]	−17.61	30.52	400	150	80
(Ph$_3$P)$_2$Pt(CH$_2$CH$_3$)$_2$[b]	16.2	15.7	700		100
Cl$_2$(bpy)PtCH$_2$CH$_2$CH$_2$[c]	−15.2	30.0	335	105	
Br$_2$(bpy)PtCH$_2$CH$_2$CH$_2$[c]	−17.9	30.4	325	110	

[a] In CH_2Cl_2 at 19 °C. Chemical shift in ppm relative to Me_4Si. [b] In CH_2Cl_2 at 35 °C. [c] From ref 34.

lowered to −51 °C, triplet and quintet features of the spectrum are wiped out, although the size of the total envelope does not increase measureably. Unfortunately, we were unable to attain the frozen spectrum, owing to limitations of solubility.[33]

The ^{13}C NMR spectrum of the platinum(II) metallacyclobutane (Ph$_3$P)$_2$PtCH$_2$CH$_2$CH$_2$ (IIa) is compared with that of the acyclic analogue (Ph$_3$P)$_2$PtEt$_2$ in Table V. The platinum(IV) metallacyclobutanes, Cl$_2$(bpy)PtCH$_2$CH$_2$CH$_2$ and Br$_2$(bpy)PtCH$_2$CH$_2$CH$_2$, previously measured by Puddephatt and co-workers,[34] are also included. Comparisons of the ^{13}C chemical shifts as well as the ^{195}Pt–^{13}C coupling constants reveal no significant differences between the platinum(II) and the platinum(IV) metallacyclobutanes. This similarity contrasts with the ^{1}H NMR spectral differences, in which the β protons in the platinum(II) and platinum(IV) structures differ substantially with respect to the chemical shifts as well as the magnitude and temperature dependence of the ^{195}Pt splittings. The latter lends support to the large β splitting arising from a direct interaction of H_β with the platinum center rather than an indirect coupling through the carbon chain.[35]

VII. Cyclic Voltammetry of Platinum(II) Metallacycles. ESR Spectra of Platinum(I) Radical Anions. The cyclic voltammetry of the various platinum(II) metallacycles and their derivatives was carried out with either an initial negative or an initial positive potential scan to examine their reductive and oxidative behavior, respectively.

Negative Potential Scan. The cathodic behavior of the platinacyclobutane I (bpy)PtCH$_2$CH$_2$CH$_2$, is illustrated by the reversible cyclic voltammogram in Figure 1. Indeed, all the bipyridine complexes of platinum(II) examined in this study exhibit a well-defined reversible wave in the initial negative scan of the cyclic voltammogram, shown in Figure 6 for the carbonyl adduct III, the dipropionyl derivative IV, and the dichloride (bpy)PtCl$_2$. The standard reduction potentials of the carbonyl derivatives III and IV listed in Table VI are significantly more positive than those of the parent platinacycle I.

When the platinacycle I is reduced at a constant potential of −1.80 V, the acetonitrile solution turns progressively redder. Integration of the current decay curve showed that 0.85 electron

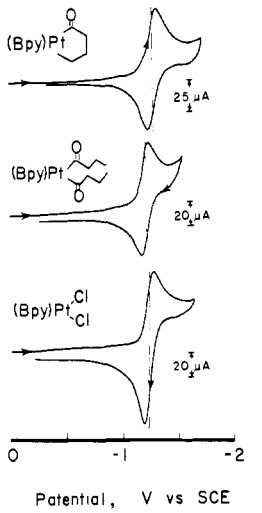

Figure 6. Initial (negative scan) cyclic voltammograms showing the reversible reduction of (upper) (bpy)PtCOCH$_2$CH$_2$CH$_2$ (III), (middle) (bpy)Pt(COCH$_2$CH$_2$CH$_3$)$_2$ (IV), (lower) (bpy)PtCl$_2$ at a scan rate of 100 mV s^{-1} in acetonitrile containing 0.1 M TEAP at 25 °C.

Table VI. Cyclic Voltammetric Parameters for the Reduction of α,α′-Bipyridine Complexes of Platinum(II) Derivatives[a]

platinum(II) complex	potentials (V vs. NaCl SCE) E_p^c	E_p^a	E°	ΔE_p
(bpy)PtCH$_2$CH$_2$CH$_2$	−1.72	−1.65	−1.68	70
(bpy)PtCOCH$_2$CH$_2$CH$_2$	−1.32	−1.24	−1.28	80
(bpy)Pt(COCH$_2$CH$_2$CH$_3$)$_2$	−1.25	−1.18	−1.22	70
(bpy)PtCl$_2$	−1.28	−1.20	−1.24	80

[a] In acetonitrile solutions containing 0.1 M TEAP at 25 °C and 100 mV s^{-1}.

(33) Further detailed investigations should quantitatively reveal the nature of the dynamic processes responsible for these temperature-dependent changes.
(34) Hall, P. W.; Puddephatt, R. J.; Tipper, C. F. H. *J. Organomet. Chem.* **1974**, *71*, 145.
(35) For a discussion of the NMR chemical shifts and coupling constants in platinacyclobutanes, see ref 34.

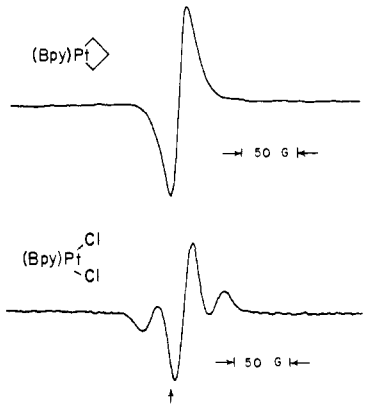

Figure 7. ESR spectra of platinum(I) anion radicals derived from the electrochemical reduction of (upper) (bpy)$\overline{PtCH_2CH_2CH_2}$ and (lower) (bpy)$PtCl_2$ in acetonitrile solutions.

Table VII. ESR Parameters of Platinum(I) Species from the Reduction of Organoplatinum(II) Complexes

platinum(II) precursor	reducing agent	line width, ΔH_{pp}, G	g value[a]	splitting, G
(bpy)$\overline{PtCH_2CH_2CH_2}$	electro[b]	14	1.98	[e]
	Na[c]	14	1.995	[e]
(bpy)$PtCl_2$	electro[d]	14	1.98	60[f]
	Na[c]	14	1.989	58[f]
(bpy)$\overline{PtCOCH_2CH_2CH_2}$	K[c]	13	1.996	
(bpy)Pt$(COCH_2CH_2CH_3)_2$	K[c]	11	1.992	~14[g]

[a] DPPH external standard (capillary). [b] Electrochemical reduction at −1.80 V vs. NaCl SCE at room temperature. [c] Alkali metal mirror reduction at room temperature. [d] Electrochemical reduction at −1.50 V. [e] Not resolved. [f] Tentatively assigned on the basis of the intensity ratio of ^{195}Pt to the other Pt isotopes. [g] Tentative assignment.

was required for each platinum. The isotropic ESR spectrum (g = 1.98) of the resultant dark red solution illustrated in Figure 7 (upper) shows no resolvable hyperfine splitting. The same spectrum is obtained in Table VII from the chemical reduction of the platinacycle I in tetrahydrofuran solution using a sodium mirror. No additional features are resolved in the frozen spectrum. The identity of the ESR spectrum obtained in different solvents and with different counterions indicates that the platinacycle radical anion is rather free and unencumbered in solution. Furthermore, we conclude from the reversible cyclic voltammogram in Figure 1 that the addition of an electron to (bpy)-$\overline{PtCH_2CH_2CH_2}$ in eq 1 occurs without attendant structural changes in the platinacycle moiety.[36,37]

The electrochemical reduction of the platinum(II) dichloride (bpy)$PtCl_2$ at −1.50 V affords a highly colored green solution. Interestingly, the ESR spectrum presented in Figure 7 (lower) shows the resolved ^{195}Pt splitting of 58 G, with the correct intensity ratio. The line width of 14 G was essentially the same as that of the platinacyclobutane anion radical.

Positive Potential Scan. The anodic behavior of platinocyclobutanes is typified by the cyclic voltammogram of $(Ph_3P)_2\overline{PtCH_2CH_2CH_2}$ showing a well-defined but irreversible wave with E_p^a = 0.61 V. No coupled cathodic wave is observed on the reverse sweep. The irreversible cathodic wave observed at the more negative potential of E_p^c = −1.00 V in Figure 8 is associated with the reduction of $(Ph_3P)_2\overline{PtCH_2CH_2CH_2}$, since the same cyclic voltammetric peak obtains in an initial negative potential scan. Such an electrochemical behavior differs from that of the carbonyl adduct III. Thus the cyclic voltammogram of III again exhibits an irreversible anodic wave with E_p^a = 0.53 V, as shown at the top of Figure 9. However, with this platinum(II) derivative, the irreversible cathodic wave with E_p^c = −0.34 is not associated with the reduction off the parent compound, which exhibits a reversible wave with E^0 at the more negative potential of −1.28 V given in Table VI and illustrated in the middle of Figure 9. The new cathodic wave is most likely to be associated with a transient product of the oxidation of III, which we suspected to be the ring-opened cation (bpy)$PtCOCH_2CH_2CH_3^+$.[38] Accordingly, the controlled potential oxidation of III was carried out at 0.60 V, and after the oxidation, chloride ion (as tetraethylammonium chloride) was added. The red solid isolated from the electrolytic mixture was tentatively identified as the monopropionylplatinum(II) chloride (bpy)Pt$(COCH_2CH_2CH_3)Cl$ (see Experimental Section). Its cyclic voltammogram at the bottom of Figure 9 shows an irreversible cathodic wave at E_p^c = −1.20 V. The shift of E_p^c from −0.34 to −1.20 V is consistent with the anation of the cation.[39]

The positive potential scan of the parent platinacyclobutane I shows a multiple anodic wave extending from about −0.3 to 0.2 V vs. NaCl SCE. On the reverse scan, no coupled cathodic wave is observed, but a new, irreversible cathodic wave appears at the more negative potential of E_p ~ −1.2 V. The latter is associated with a product of the oxidation of I, since it is absent in the initial negative potential scan of I. Controlled potential oxidation of I at 0 V yielded 0.74 electron per platinum. No cyclopropane or other C_3 hydrocarbon gas was liberated during the electrolysis.

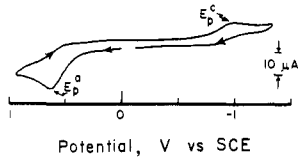

Figure 8. Initial (positive potential) scan cyclic voltammogram of $(Ph_3P)_2\overline{PtCH_2CH_2CH_2}$ at a sweep rate of 100 mV s^{-1} in acetonitrile containing 0.1 M TEAP at 25 °C. The same CV is obtained in an initial negative potential scan.

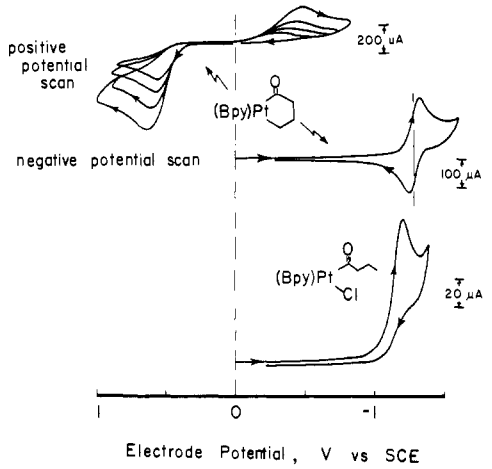

Figure 9. Cyclic voltammograms of the carbonyl adduct (bpy)-$\overline{PtCOCH_2CH_2CH_2}$ III at an initial positive potential scan at 100, 200, 400, and 800 mV s^{-1} (upper), and at an initial negative potential scan at 100 mV s^{-1} (middle). The CV of (bpy)Pt$(COCH_2CH_2CH_3)Cl$ obtained by the oxidation of III, as described in the text, is described in the lower figure.

(36) Within the electrochemical time scale of ~1 to 10 s.[37]
(37) Bard, A. J.; Faulkner, L. R. "Electrochemical Methods"; Wiley: New York, 1980.

(38) Formed by ring opening of the platinum(III) species followed by hydrogen abstraction from the solvent, see Discussion. An alternative possibility is that the oxidation of III and the reduction of the product are kinetically slow.
(39) The reduction potentials of cations are generally more positive than the corresponding neutral species.

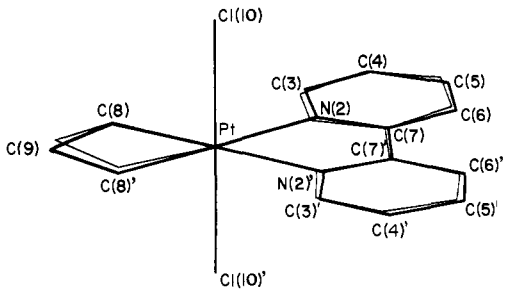

Figure 10. Structural comparison of the platinum(II) and platinum(IV) metallacyclobutane moieties. Heavy lines are drawn to $\overline{CH_2CH_2CH_2}Pt(bpy)Cl_2$ and the lighter lines are drawn to $\overline{CH_2CH_2CH_2}Pt(bpy)$ after the superposition of the platinum centers.

Table VIII. Comparative Structural Parameters of Platinum(II) and Platinum(IV) Metallacyclobutanes[a]

bond length or angle	(bpy)Pt	Cl (bpy)Pt Cl
Pt-C_α, Å	2.03 (1)	2.07 (4)
C_α-C_β, Å	1.53 (1)	1.63 (6)
C_α-Pt-C_α, deg	69.9 (4)	72 (2)
Pt-C_α-C_β, deg	95.5 (5)	95 (5)
C_α-C_β-C_α, deg	98.8 (8)	96 (5)
Pt-N, Å	2.105 (8)	2.20 (3)
Pt-Cl, Å		2.23 (3)

[a] Numbers in parentheses refer to the error in the least significant digit.

The other platinum(II) complexes examined in this study, $(bpy)Pt(COCH_2CH_2CH_3)_2$ and $(bpy)PtCl_2$, showed well-defined but irreversible anodic waves at E_p^a = 1.01 and 1.51 V, respectively.

Discussion

The cathodic and chemical reductions of the platinum(IV) metallacyclobutane $Cl_2(bpy)\overline{PtCH_2CH_2CH_2}$ both proceed via the facile reductive elimination of the pair of axial chlorine ligands, leaving the platinacyclobutane moiety intact. The overall transformation is reversible, since the treatment of the platinum(II) product $(bpy)\overline{PtCH_2CH_2CH_2}$ with chlorine regenerates the original platinacyclobutane,[40] i.e.,

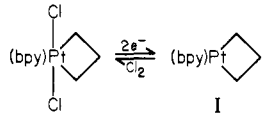

(13)

I

Indeed, the close similarity between these skeletal fragments is illustrated by the overlapping structures shown in the perspective in Figure 10. The comparison of the pertinent bond angles and bond distances given in Table VIII indicates that the oxidative addition of chlorine to I occurs with minimal structural reorganization. The degree of the puckering of the platinacycle ring in the crystals of both analogues is rather small, the flap angle defined by the planes $C_\alpha C_\beta C_\alpha$ and $C_\alpha PtC_\alpha$ being only 3° in I and 0° in $Cl_2(bpy)\overline{PtCH_2CH_2CH_2}$ (fixed by crystallographic symmetry). The transannular distance Pt-C_β (2.67 (1) Å in I and 2.76 (4) Å in the platinum(IV) analogue) is essentially the same in both platinacyclobutanes.

Considering the structural integration of the bipyridine ligand with the platinacyclobutane moiety in the description above, it is rather easily replaced in I by various phosphine ligands and to a lesser degree by *tert*-butyl isocyanide in eq 7–9. The ready insertion of sulfur dioxide as well as carbon monoxide into the platinum–carbon as described in eq 10 and 12 also suggests that associative pathways are readily available for the coordinatively unsaturated platinacyclobutane I, which we formulate in the following composite scheme:[41]

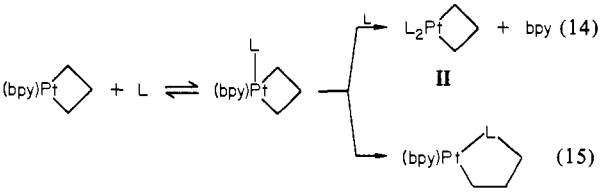

III, V

Such facile substitution and insertion reactions of I contrast with the inert behavior of the coordinatively saturated platinum(IV) metallacyclobutane $Cl_2(bpy)\overline{PtCH_2CH_2CH_2}$ under comparable experimental conditions.[15] Furthermore, in the platinum(IV) analogue, the addition of phosphines induces the reductive elimination of the trimethylene ligand and not the simple replacement of pyridine, i.e.,

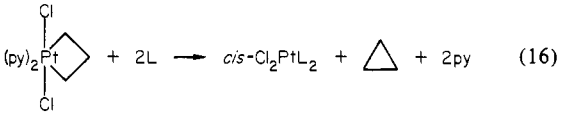

(16)

where L = Ph_3P, Ph_3As, and Ph_3Sb.[42,43] The α,α'-bipyridine derivative of the platinum(IV) metallacyclobutane is only slowly decomposed by triphenylphosphine.[42] The synthesis of the phosphine derivatives of the platinum(IV) metallacyclobutane, e.g., $Cl_2(Ph_3P)_2Pt(CH_2)_3$, can be effected by the ready oxidative addition of chlorine to the corresponding platinum(II) metallacyclobutane IIb. (Compare eq 13.)

The difference between metallacyclobutane moieties in the platinum(II) and the platinum(IV) complexes is also shown in the ^1H NMR spectra. For example, in the platinum(IV) metallacyclobutane $Cl_2(py)_2\overline{PtCH_2CH_2CH_2}$, the coupling constant for the protons α to platinum is reported to be 83 Hz, and the β couplings are unresolved.[22] By comparison, in the platinum(II) analogue I, the corresponding α and β coupling constants are 115 and 110 Hz, respectively. Moreover, in the phosphine derivatives IIa–c, the β coupling constants are substantially larger than the α coupling constants in Table IV. The long-range coupling of $J_{P\text{-}H}$ = 4.3 Hz for the β protons to the phosphorus nucleus in $(Et_3P)_2\overline{PtCH_2CH_2CH_2}$ (IIc) is also unusually large. These observations raise the possibility of a facile dynamic puckering motion in solution allowed by a rather strain-free, 4-membered ring,[44] e.g.,

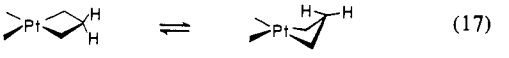

(17)

Such changes are consistent with the difference in the ^1H and ^{13}C NMR spectral parameters in Table IV and V as well as with the temperature dependence of the β proton coupling to the platinum center in Figure 5.[33]

Since the Pt–C bonds are longer than C–C bonds, the ring strain in platinacyclobutanes is expected to be less than that in cyclobutane.[18] Indeed, the ring strain in the platinacyclobutane $(Et_3P)_2\overline{PtCH_2C(CH_3)_2CH_2}$ is only ≤5 kcal mol^{-1} greater than that in the platinacyclopentane analogue.[44] Furthermore, an

(40) The oxidative addition of chlorine to *cis*-$Me_2Pt(PEt_3)_2$ also affords the trans adduct. Chatt, J.; Shaw, B. L. *J. Chem. Soc.* **1959**, 705, 4020. Note that iodine leads to cleavage (compare ref 25).

(41) To substantiate this scheme, kinetic studies are in progress and will be reported at a later time.

(42) Hall, P. W.; Puddephatt, R. J.; Tipper, C. F. H. *J. Organomet. Chem.* **1975**, *84*, 407.

(43) Perkins, D. C. L.; Puddephatt, R. J.; Rendle, M. C.; Tipper, C. F. H. *J. Organomet. Chem.* **1980**, *195*, 105.

(44) Moore, S. S.; DiCosimo, R.; Sowinski, A. F.; Whitesides, G. M. *J. Am. Chem. Soc.* **1981**, *103*, 981.

estimate of the Pt–C bond strength in $Cl_2(py)\overline{PtCH_2CH_2CH_2}$ is given as 28 kcal mol^{-1}, which compares with 34 kcal mol^{-1} for the Pt–C bond in the closest available relative, viz., $Me_3Pt(PMe_2Ph)_2I$.[45] Studies of the decomposition of the platinacyclobutane I support the notion of its thermal stability. Thus, it is only half decomposed after 4 h at 60 °C in acetonitrile to afford ethylene as well as propylene and some cyclopropane, but we hasten to add that the thermolytic behavior of I appears to be highly dependent on its purity.[46] However ethylene is generated in the thermal decomposition of I, it is also an important fragment in the mass spectral cracking upon electron impact at 40 eV in the gas phase. When the platinacyclobutane I is vaporized at an inlet temperature of 55 °C, ethylene is the principal fragment ion, the ratio of the abundances of $C_2H_4^+$ to $C_3H_6^+$ being 7, which decreases as the inlet temperature is raised. Unfortunately, the platinum-containing species are only measureable at the higher temperatures. At 120 °C, the parent ion $(bpy)\overline{PtCH_2CH_2CH_2}^+$ with m/e 393 (^{195}Pt), the parent – ethylene ion $(bpy)PtCH_2^+$ with m/e 365 (^{195}Pt), and the parent – propylene ion $(bpy)Pt^+$ with m/e 351 (^{195}Pt) are observed in the relative abundances of 32:15:51. Such fragmentations of ethylene from the platinacyclobutanes suggest that the structural reorganization of the methylene groups may also be facile, in perhaps a manner akin to the isomerization of the platinum(IV) analogues.[47,48] (Although we have already carried out some such studies, the problems associated with the *rigorous* purification of these platinacyclobutanes mentioned above[46] discourages us from reporting our results at this time.)

Despite the thermal stability of the platinacyclobutane I, its stability to either oxidation or reduction is quite limited. For example, the exposure to air leads to degradation.[49] Furthermore, the electrochemical oxidation described in the cyclic voltammagram of I is consistent with a highly unstable cation, $(bpy)\overline{PtCH_2CH_2CH_2}^+$, which decomposes without the liberation of any C_2 or C_3 hydrocarbon gases. The homolytic fragmentation of one Pt–C bond in eq 18b,[50] derives from the behavior of analogous

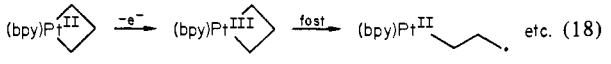

etc. (18)

dialkylplatinum(III) species which we examined earlier.[51] Subsequent abstraction of hydrogen from the solvent (acetonitrile) is facile[52] and would generate the propylplatinum(II) cation $(bpy)PtCH_2CH_2CH_3^+$. Such a hydrogen transfer occurs in the cleavage of the carbonyl adduct $(bpy)\overline{PtCOCH_2CH_2CH_2}$, which ultimately leads to the dipropionylplatinum(II) complex IV in eq 11.[53]

The chemical as well as electrochemical reductions of the platinum(II) metallacyclobutane and its derivatives in Table VI afford paramagnetic platinum(I) species. These anion radicals are persistent but not sufficiently long-lived to enable us to isolate them in crystalline form. Serious attempts to resolve the proton hyperfine splittings in the ESR spectrum of the platinacyclobutane anion radical have been futile, probably owing to the large nitrogen quadrupole moment in the bipyridine ligand. Consequently, we are unable to describe the electron delocalization into the platinacycle moiety at this time.

Summary and Conclusions

A variety of coordinatively unsaturated platinum(II) metallacyclobutanes are conveniently synthesized from the reductions of easily accessible platinum(IV) precursors such as $Cl_2(bpy)\overline{PtCH_2CH_2CH_2}$. The structural relationship of platinum(II) and platinum(IV) metallacyclobutanes is pointed out by the X-ray crystallographic comparisons of $\overline{CH_2CH_2CH_2Pt^{II}}(bpy)$ and $\overline{CH_2CH_2CH_2Pt^{IV}}(bpy)Cl_2$, respectively. The platinacyclobutane $(bpy)\overline{PtCH_2CH_2CH_2}$ (I) undergoes two facile classes of reactions: (1) replacement of the α,α'-bipyridine ligand by monodentate ligands and (2) insertion into the Pt–C bond of the metallacycle by CO and SO_2. Preliminary studies have shown that a variety of electrophiles, including alkyl halides and peroxo and metal complexes, also react easily with these relatively electron-rich platinacycles. Reduction and oxidation of the platinum(II) centers carried out electrochemically reveal the existence of persistent platinum(I) anion radicals and metastable platinum(III) species, respectively, which potentially offer more rich chemistry of metallacycles.

Experimental Section

Materials. The platinum(IV) metallacyclobutanes $Cl_2(bpy)\overline{PtCH_2CH_2CH_2}$, $Cl_2(Ph_2phen)\overline{PtCH_2CH_2CH_2}$, and $Cl_2(py)_2\overline{PtCH_2CH_2CH_2}$ were prepared from H_2PtCl_6, cyclopropane, and the appropriate ligand by the methods described by Adams et al.[22,54] $(Bpy)PtCl_2$ was prepared from chloroplatinic acid and α,α'-bipyridine.[55] The phosphines were obtained from Pressure Chemical Co. and used directly. Reagent grade acetonitrile (Mallinckrodt Chemical Co.) was initially purified by fractional distillation from calcium hydride through an 18-stage bubble plate (Oldershaw) column. It was stirred with a mixture of $KMnO_4$ and Na_2CO_3 (10 g L^{-1} of each) for 24 h and then filtered. After bulb-to-bulb distillation, it was redistilled from P_2O_5, follow by CaH_2.

Electrochemical Measurements. Electrochemistry was performed on a Princeton Applied Research Model 173 potentiostat which allows the electrolysis to be performed under conditions of constant potential or constant current. The potentiostat was equipped with a Model 176 current-to-voltage converter which provided a feedback compensation for ohmic drop between the working and reference electrodes. The voltage follower amplifier (Model 178) was mounted external to the potentiostat with a minmum length of high impedance connection to the reference electrode. This arrangement ensured low noise pickup. Cyclic voltammograms were recorded on a Houston Series 2000 X-Y recorder. For sweep rates greater than 1 V s^{-1}, the voltammograms were recorded on a Princeton Applied Research Model 4102 transient signal recorder. The electrochemical cell was constructed according to the design of Van

(45) (a) Hall, P. W.; Puddephatt, R. J.; Seddon, K. R.; Tipper, C. F. H. *J. Organomet. Chem.* **1974**, *81*, 423. (b) Brown, M. P.; Puddephatt, R. J; Upton, C. E. E. *J. Chem. Soc., Dalton Trans.* **1974**, 2457.

(46) (a) For example, the sample from which the crystal structure shown in Figure 2 was obtained yielded ethylene (20%), propylene (40%), and cyclopropane (12%) on thermal decomposition in acetonitrile. However, a much more highly purified sample of I afforded propylene (70%) and cyclopropane (19%), but only small amounts of ethylene (1%). The purer sample also decomposed more slowly. These results suggest that there are several competing pathways for the thermolytic decomposition of the platinacyclobutane I, the relative importance of which are affected by trace impurities. Further kinetic studies are pending the resolution of this very difficult technical problem. (b) The completed studies will be reported separately.

(47) Al-Essa, R. J.; Puddephatt, R. J.; Quyser, M. A.; Tipper, C. F. H. *J. Am. Chem. Soc.* **1979**, *101*, 364. Al-Essa, R. J.; Puddephatt, R. J.; Thompson, P. J.; Tipper, C. F. H. *Ibid.* **1980**, *102*, 7546.

(48) Casey, C. P.; Scheck, D. M.; Shusterman, A. J. *J. Am. Chem. Soc.* **1979**, *101*, 4233.

(49) The rate of aerial decomposition of I is also highly dependent on its purity, as initially noted in ref 46.

(50) For the photolytic generation of such a radical from the platinum(IV) analogue, see: Perkins, D. C. L.; Puddephatt, R. J.; Tipper, C. F. H. *J. Organomet. Chem.* **1978**, *154*, C16; **1980**, *186*, 419.

(51) Chen, J. Y.; Kochi, J. K. *J. Am. Chem. Soc.* **1977**, *99*, 1450.

(52) Nonhebel, D. C.; Walton, J. C. "Free Radical Chemistry"; Cambridge University Press: London, 1974; p 239 ff.

(53) We would formulate such a transformation by the following sequence of intermediates:

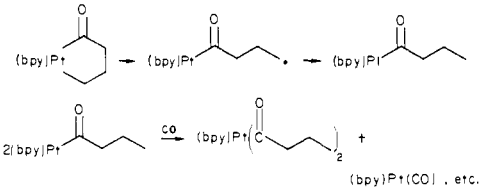

Deuterium labeling studies would obviously be desirable.

(54) Cf. Littlecott, G. W.; McQuillin, F. J.; Powell, K. G. *Inorg. Synth.* **1976**, *16*, 113.

(55) Morgan, G. T.; Burstall, F. H. *J. Chem. Soc.* **1934**, 965.

Duyne and Reilley.[56] The distance between the platinum working electrode and the tip of the salt bridge was 1 mm to ensure a minmum ohmic drop. The positive feedback compensation was set by initially applying a chronoamperometric step in a region where there was no electrode process. The amount of feedback was then optimized to minimize the response time in the absence of ringing. For the electrochemical cells employed in this study, this typically required 1% or less feedback of the current.

The cyclic voltammograms of the organometals were examined at 25 °C in acetonitrile solutions containing 0.1 M tetraethylammonium perchlorate (TEAP). The stationary platinum microelectrode was routinely cleaned by soaking it in concentrated nitric acid, followed by repeated rinsing in distilled water and drying at 120 °C prior to use with each organometal. The anodic peak potentials were always reproducible to within 50 mV, and repeated CV scans did not affect the appearance of the voltammograms.

Electrochemical Synthesis of (bpy)$\overline{PtCH_2CH_2CH_2}$ (I). The electrolysis cell was charged with 100 mg of $Cl_2(bpy)PtC_3H_6$ and 10 mL of acetonitrile containing 0.1 M TEAP. The mixture was cooled to 0 °C and electrolyzed at −1.35 V. The initial pale yellow solution slowly turned dark orange, as the $Cl_2(bpy)PtC_3H_6$ dissolved and was reduced. Integration of the resultant current decay curve gave 48.6 C or 1.98 ± 0.05 electrons per Pt. Addition of 5 mL of degassed toluene resulted in the precipitation of the supporting electrolyte, which was separated by filtration. The solvent was removed in vacuo from the filtrate, and the resultant orange solid redissolved in pure acetonitrile. Cooling the solution to −20 °C afforded 63 mg of orange crystals. The compound gradually turned black on heating and gave no definite melting point. Anal. Calcd for $PtC_{13}H_{14}N_2$: C, 39.70; H, 3.58; N, 7.12. Found: C, 40.04; H, 3.56; N, 7.40.

Synthesis of (bpy)$\overline{PtCH_2CH_2CH_2}$ by Chemical Reduction. An approximately 0.2 wt % sodium amalgam was prepared and standardized by quenching with distilled water, followed by titration of the alkali with a standard HCl solution. A mixture of 500 mg (1.07 mmol) of $Cl_2(bpy)PtC_3H_6$ and 100 mL of acetonitrile at 0 °C was treated by the dropwise addition of Na amalgam over a 4-h period (2.2 equiv of Na total). The solution was filtered and the filtrate cooled to −20 °C for 8 h to yield orange crystals, which upon recrystallization from acetonitrile yielded 300 mg of I. The IR spectrum is characterized by two sharp bands at 2900 and 2880 cm^{-1} in the C–H stretching region.

Preparation of $(Ph_3P)_2\overline{PtCH_2CH_2CH_2}$. The electrolysis cell was charged with 0.10 g (0.22 mmol) of $Cl_2(bpy)PtC_3H_6$ and 10 mL of acetonitrile containing 0.1 M TEAP. After the reduction at −1.35 V, 0.20 g (0.75 mmol) of Ph_3P dissolved in acetonitrile was added to the catholyte. The color of the solution lightened immediately upon the addition of Ph_3P, and pale yellow crystals separated over a period of 15 min. These were recrystallized twice by dissolution in methylene chloride followed by the addition of ethanol to afford 150 mg of white needles, mp 142–143 dec. Anal. Calcd for $PtC_{39}H_{36}P_2$: C, 61.49; H, 4.76; P, 8.13. Found: C, 61.69; H, 4.88; P, 8.31.

Preparation of $(Et_3P)_2\overline{PtCH_2CH_2CH_2}$ (IIb and IIc). A mixture of 100 mg (0.25 mmol) of $bpyPtC_3H_6$ and 10 mL of acetonitrile was cooled to 0 °C, and 0.1 mL of neat Et_3P was added. The solution turned almost colorless immediately upon the addition of the phosphine. The solvent was removed in vacuo, and a cold finger cooled with dry ice was inserted into the flask. The displaced bpy was sublimated in vacuo, keeping the flask at room temperature. The tan residue was recrystallized twice from pentane to yield 20 mg of IIb. The same procedure was used to prepare the trimethylphosphine derivative, except for the isolation, which involved removal of the solvent in vacuo, followed by extraction of the solid residue with pentane. Cooling the pentane extract at −20 °C afforded white crystals. After recrystallization 4 more times from pentane, 50 mg of IIc was obtained.

Preparation of $(t\text{-BuNC})_2\overline{PtCH_2CH_2CH_2}$ (IId). A solution of 100 mg (0.25 mmol) of $(bpy)PtC_3H_6$ in 20 mL of CH_3CN was treated with 0.1 mL of *tert*-butyl isocyanide. There was no color change apparent. The solution was stirred for 4 h at room temperature, during which the orange color lightened only somewhat. The solvent was removed in vacuo and the residue extracted with pentane. The pentane extracts, upon cooling to −20 °C, yielded yellow crystals, which were recrystallized twice from pentane to yield 20 mg of white needles. Anal. Calcd for $PtC_{13}H_{24}N_2$: C, 38.70; H, 6.00; N, 6.94. Found: C, 38.71; H, 6.26; N, 6.89.

Preparation of (bpy)$\overline{PtCOCH_2CH_2CH_2}$ (III). A mixture of 150 mg of $(bpy)PtC_3H_6$ and 10 mL of CH_3CN was stirred at ambient temperatures under 1 atm of carbon monoxide for 4 h. There was a gradual darkening of the solution, which became noticeable only after 15 min. After 4 h, the solution was brown and homogeneous. The solvent was removed in vacuo and the dark residual solid extracted repeatedly with small amounts of toluene until the extracts were no longer orange. A dark green residue remained (vide infra). The combined extracts were concentrated in vacuo, and the resultant orange solid was chromatographed with acetone under argon with a 3-ft alumina column. The first orange band was concentrated in vacuo, and the addition of ether afforded orange crystals. Recrystallization from a mixture of acetone and ether yielded 80 mg of orange needles. Anal. Calcd for $PtC_{14}H_{14}N_2O$: C, 39.90; H, 3.35; N, 6.65. Found: C, 39.85; H, 3.48; N, 6.89.

Preparation of $(bpy)Pt(COCH_2CH_2CH_3)_2$ (IV). The reaction of $(bpy)PtC_3H_6$ with CO always yields some IV as one of the products even at short reaction times. In order to optimize the yield of IV, we simply carried out the reaction for longer periods. For example, a solution of 100 mg of $(bpy)PtC_3H_6$ in 20 mL of CH_3CN was stirred at room temperature under 1 atm of CO. The mixture undergoes a series of color changes, beginning with a darkening after 15 min, going through a second stage where it appears brownish, and eventually becoming a deep green. After stirring for 48 h, the solvent was removed in vacuo and the black residue extracted repeatedly with small portions of toluene until the extracts were colorless. The combined extracts were concentrated in vacuo, and the red residue was dissolved in methylene chloride. Addition of ether afforded 20 mg of red needles; IR 1590, 1620 cm^{-1}. A crystal was grown from acetone to yield the structure shown in Figure 4. The black residue was dissolved in acetone, which upon cooling yielded a dark green powder. Attempts to obtain crystalline material were unsuccessful. There were two strong IR bands at 1860 and 2050 cm^{-1}, and weak bpy resonance was observed in the ^1H NMR spectrum of the green powder. Bipyridine bands were also evident in the IR spectrum of a KBr pellet. The material was not investigated further.

Anodic Oxidation of (bpy)$\overline{PtCOCH_2CH_2CH_2}$ (III). A solution of 15 mg of (bpy)$\overline{PtCOCH_2CH_2CH_2}$ (III) in 20 mL of CH_3CN was oxidized at 0.6 V. After the oxidation, a solution of 50 mg of Et_4NCl was added. The CV of the resulting solution showed a new irreversible cathodic wave at −1.20 V (compared with −0.43 V in III). The solvent was removed in vacuo, and the residue was extracted with methylene chloride. Concentration of the extract and the addition of ether resulted in the precipitation of a red solid, which was recrystallized from the same solvent pair. The ^1H NMR spectrum, in addition to the bpy resonances, shows the propionyl ligand as consisting of three sets of resonances at δ 3.97, 2.71, and 1.37, which are shifted to lower fields relative to these in IV (see Table IV). We tentatively assign the structure of the oxidation product to $(bpy)Pt(COCH_2CH_2CH_3)Cl$.

Preparation of $(Me_3P)_2\overline{PtSO_2CH_2CH_2CH_2}$. A solution of 100 mg of $(bpy)PtC_3H_6$ in 10 mL of pentane was degassed by successive freeze–pump–thaw cycles and finally cooled to 0 °C. SO_2 (1 atm) was condensed into the flask on a vacuum line. A yellow precipitate separated from the solution over a 5-min period. The solvent was removed in vacuo and the solid recrystallized 3 times from CH_3CN to yield 50 mg of white needles. Anal. Calcd for $PtC_9H_{24}P_2SO_2$: C, 23.84; H, 5.33. Found: C, 24.10; H, 5.63. The bpy analogue, $(bpy)PtC_3H_6$, in acetonitrile also reacted rapidly with SO_2 to afford a flash of green color, which faded within 1 min to yield a pale yellow solution and an insoluble yellow precipitate.

Oxidation of (bpy)$\overline{PtCH_2CH_2CH_2}$ with Chlorine. A solution of 20 mg (0.051 mmol) of (bpy)$\overline{PtCH_2CH_2CH_2}$ in 20 mL of CH_3CN was prepared under argon in a flask equipped with a side arm and stopcock. When 1 equiv (1.1 mL) of chlorine gas was added above the solution, the dark orange color was immediately dispelled, leaving a pale yellow solution. The cyclic voltammogram of a 1-mL aliquot of this solution (after the addition of TEAP) exhibited the cathodic wave at −1.35 V corresponding to the first reduction wave of $Cl_2(bpy)PtC_3H_6$. Comparison of the peak current with that of an authentic solution of $Cl_2(bpy)PtC_3H_6$ indicated a quantitative yield (±10%). Removal of the solvent from the remainder (19 mL) of the solution in vacuo afforded a light yellow solid whose IR spectrum (KBr) was the same as that of authentic $Cl_2(bpy)PtC_3H_6$ in all respects.

A sample of 32.9 mg or 0.043 mmol of $(Ph_3P)_2PtC_3H_6$ (IIa) was treated with chlorine by allowing 1 equiv of the gas to stand over the solid for 10 min. The resultant solid was dissolved in methylene chloride, and the addition of ethanol yielded light yellow microcrystals over a period of 10–15 min. Recrystallization from the same solvent 3 times yielded material melting at 257–259 °C dec. The ^1H NMR spectrum showed an unresolved singlet resonance at δ 1.51 (6 H) for the methylene protons and a multiple resonance between δ 7.47 and 7.81 (30 H) for the triphenylphosphine ligands.

(56) Van Duyne, R. P.; Reilley, C. N. *Anal. Chem.* **1972**, *44*, 142.

Spectrometers. The ESR measurements were carried out on a Varian E4 spectrometer using a capillary containing DPPH as an external standard. The platinum(I) species in Table VII were prepared electrochemically or by alkali metal reduction by procedures described earlier.[57,58] The ^{1}H NMR spectra were recorded on either a Varian HR 220 (phosphorus decoupling) or a T60 spectrometer. The ^{13}C and ^{31}P NMR spectra were obtained on a Varian XL 100 spectrometer.

X-ray Crystallography. General Data. The diffractometer used in this study consisted of a Picker goniostat interfaced to a T1980B minicomputer with 56K words of 16-bit memory. The angle drives of the goniostat were interfaced by using Slo-Syn stepping motors and translator driver boards. The computer is programmed to operate on an interrupt basis by using a precision internal clock, and the scan speeds are controlled by the pulse rate delivered to the translator driver boards. Each pulse will drive the corresponding goniostat angle 0.005°, and virtually any angular rate can be chosen. A "filter attenuator wheel", mounted on the detector arm, is positioned such that up to 20 apertures or attenuators can be automatically located in the diffraction beam path. Apertures are provided for automatic top/bottom-left/right centering of reflections, and these are utilized for both goniostat and crystal alignment. Standard "NIM-bin" electronics are used for pulse shaping and energy discrimination, and the computer-controlled timer and scaler were constructed locally. Reflection data are collected in a normal θ–2θ scan mode with backgrounds at each extreme of the scan. A buffer is provided so that up to 4800 reflection data can be stored in the computer memory.

A liquid nitrogen boil-off cooling system is used to maintain samples at −140 to −180 °C. The system consists of two 30-L storage Dewars to supply the dry nitrogen gas for the cold stream and concentric warm stream and a third 30-L recooling Dewar through which the cooling gas is passed. The recooling Dewar consists of a coil (2-m length) of copper tubing that is joined to an evacuated and silvered glass delivery tube. The delivery tube is designed to supply the cold nitrogen in a fixed position from the bottom of the χ circle. The exit nozzle is carefully streamlined to ensure a laminar flow. Thermocouples and heating wires located in the exit nozzle monitor and control the temperature. Short-term temperature fluctuation is typically ±0.2 °C with long-term stability of ±3 °C. Crystals are mounted on glass fibers by using a silicon grease, which remains amorphous and becomes rigid at the normal operating temperature of the system.

Data are reduced by using the equations $I = C - 0.5(t_c/t_b)(B_1 + B_2)$ and $\sigma(I) = [C + 0.25(t_c/t_b)^2(B_1 + B_2) + (pI)^2]^{1/2}$, where C is the total integrated peak count obtained in scan time t_c, B_1 and B_2 are the background counts obtained in time t_b, and p is the "ignorance factor". The function minimized in the least-squares program is $\sum w|F_o - F_c|^2$ where $w = 1/\sigma(F_o)$, and residuals are defined as $R(F) = \sum||F_o| - |F_c||/\sum|F_o|$ and $R_w(F) = (\sum w||F_o| - |F_c||^2/\sum wF_o^2)^{1/2}$.

(bpy)PtCH$_2$CH$_2$CH$_2$. A well-formed parallelopiped of maximum dimension 0.16 mm was used. A search of a limited hemisphere of reciprocal space revealed a monoclinic cell, $P2_1/c$, with a = 7.122 (2) Å, b = 9.830 (3) Å, c = 16.130 (5) Å, and β = 94.59 (1)° at −170 °C, on the basis of a least-squares refinement of angular data from 64 reflections. The cell volume of 1125.5 (1) Å^3 gives a density of 2.321 g cm^{-3} for Z = 4. Data were collected (Mo K$_\alpha$, graphite monochromator, λ = 0.71069 Å) for 5° ≤ 2θ ≤ 50° by using a continuous θ–2θ scan with the following parameters: 4.0° min^{-1} scan speed; 2.0°+ dispersion width; 5-s stationary backgrounds at each extreme of the scan; detector to sample distance of 22.5 cm; sample to source distance of 23.5 cm; and takeoff angle of 2.0°.

A total of 2357 reflections were collected, including redundancies. Of the 1999 unique data, 1749 had $F \geq 2.33\sigma(F)$ and were used in the refinement. Manual ψ scans indicated an absorption correction was necessary (μ = 125.7 cm^{-1}), and the minimum and maximum transmission coefficients were 0.173 and 0.405, respectively.

The structure was solved by a combination of Patterson techniques, direct methods (LSAM), and Fourier techniques. A difference Fourier synthesis phased on the refined nonhydrogen coordinates clearly located all hydrogen atoms. Full-matrix refinement included isotropic thermal parameters (Table IX) for hydrogen atoms and anisotropic parameters for nonhydrogens as well as positional parameters and an overall scale factor. Final residuals were $R(F)$ = 0.036 and $R_w(F)$ = 0.037. The goodness of fit for the last cycle was 1.002, and the maximum shift/error was 0.05. The final difference Fourier synthesis indicated a residue of 2.5 e Å^{-3} adjacent to the Pt, and all other peaks were less than 0.7 e Å^{-3}.

Table IX. Fractional Coordinates and Isotropic Thermal Parameters[a]

atom	x	y	z	B_{iso}
		A. (bpy)PtCH$_2$CH$_2$CH$_2$		
Pt(1)	2102 (1)	2715.7 (3)	3767.2 (2)	11
N(2)	3737 (12)	2086 (8)	4845 (5)	14
C(3)	3211 (15)	1097 (10)	5358 (7)	18
C(4)	4392 (16)	643 (10)	6010 (6)	17
C(5)	6150 (14)	1237 (11)	6163 (6)	15
C(6)	6664 (15)	2280 (10)	5657 (6)	17
C(7)	5427 (14)	2695 (10)	4997 (7)	15
C(8)	5836 (13)	3767 (10)	4414 (6)	14
C(9)	7447 (15)	4559 (10)	4463 (7)	19
C(10)	7725 (15)	5527 (10)	3848 (7)	18
C(11)	6357 (15)	5696 (11)	3214 (7)	19
C(12)	4755 (15)	4910 (10)	3201 (6)	15
N(13)	4491 (12)	3972 (7)	3760 (5)	14
C(14)	422 (15)	3199 (12)	2733 (6)	16
C(15)	−1083 (14)	2119 (10)	2859 (7)	16
C(16)	−253 (14)	1531 (10)	3691 (6)	15
H(17)	218 (15)	78 (10)	527 (6)	10 (21)
H(18)	416 (18)	2 (12)	628 (8)	29 (29)
H(19)	680 (15)	91 (10)	651 (6)	15 (23)
H(20)	803 (14)	253 (8)	576 (5)	0 (17)
H(21)	879 (22)	443 (16)	488 (9)	73 (44)
H(22)	866 (16)	595 (10)	388 (6)	10 (23)
H(23)	659 (15)	634 (11)	274 (7)	23 (24)
H(24)	408 (18)	497 (13)	278 (7)	32 (30)
H(25)	92 (12)	341 (9)	222 (5)	0 (16)
H(26)	12 (22)	402 (16)	264 (9)	52 (40)
H(27)	−241 (14)	248 (8)	289 (5)	0 (17)
H(28)	−121 (14)	145 (11)	256 (6)	14 (22)
H(29)	−16 (12)	38 (8)	376 (5)	0 (16)
H(30)	−95 (12)	171 (9)	411 (5)	0 (16)
		B. Cl$_2$(bpy)PtCH$_2$CH$_2$CH$_2$		
Pt(1)	250*	250*	343.9 (2)	43
N(2)	358 (2)	250*	464 (3)	48
C(3)	967 (3)	250*	45 (3)	93
C(4)	965 (3)	250*	532 (3)	35
C(5)	16 (4)	250*	619 (3)	38
C(6)	125 (3)	250*	624 (3)	42
C(7)	189 (3)	250*	544 (3)	43
C(8)	348 (3)	250*	229 (3)	50
C(9)	250*	250*	155 (6)	64
Cl(10)	250*	960 (3)	343 (1)	72
		C. (bpy)Pt(COCH$_2$CH$_2$CH$_3$)$_2$[b]		
Pt(1)	−1745.0 (4)	4940.4 (5)	1517 (1)	16
N(2)	−1004 (10)	3755 (9)	1899 (21)	21
C(3)	−1270 (12)	2899 (12)	1663 (26)	20
C(4)	−756 (14)	2172 (12)	1862 (28)	27
C(5)	91 (12)	2324 (13)	2183 (28)	25
C(6)	372 (13)	3176 (12)	2272 (28)	24
C(7)	9838 (13)	3916 (13)	2231 (29)	23
C(8)	71 (10)	4874 (11)	2468 (21)	13
C(9)	883 (11)	5134 (14)	3057 (26)	28
C(10)	1049 (12)	6052 (16)	3317 (28)	32
C(11)	411 (11)	6675 (12)	2980 (27)	18
C(12)	−355 (12)	6353 (14)	2459 (25)	20
N(13)	−537 (9)	5478 (10)	2231 (19)	15
O(14)	−3201 (8)	3951 (9)	2136 (19)	25
C(15)	−2813 (11)	4336 (12)	933 (28)	24
C(16)	−3162 (12)	4302 (16)	−1110 (28)	33
C(17)	−4028 (13)	4014 (16)	−1431 (37)	42
C(18)	−4286 (16)	4045 (21)	−3464 (40)	62
O(19)	−2097 (8)	6719 (9)	166 (19)	27
C(20)	−2326 (11)	6124 (13)	1100 (26)	18
C(21)	−3144 (14)	6266 (13)	2186 (34)	33
C(22)	−3030 (13)	6127 (15)	4272 (30)	31
C(23)	−2430 (13)	6798 (15)	5182 (30)	35

[a] Fractional coordinates are ×10^4 for nonhydrogen atoms and ×10^3 for hydrogen atoms. B_{iso} values are ×10. Isotropic values for those atoms refined anisotropically are calculated using the formula given by: Hamilton, W. C. *Acta Crystallogr.* 1959, *12*, 609. Parameters marked by an asterisk were not varied. [b] For the fractional coordinates and isotropic thermal parameters of the hydrogens, see supplementary material, Table XIII.

(57) Klingler, R. J.; Huffman, J. C.; Kochi, J. K. *Inorg. Chem.* **1981**, *20*, 34.

(58) Kwan, C. L.; Carmack, M.; Kochi, J. K. *J. Phys. Chem.* **1976**, *80*, 1786.

$Cl_2(bpy)\overline{PtCH_2CH_2CH_2}$. Nearly all crystals obtained were either twinned or split. A single crystal (0.02 × 0.04 × 0.20 mm) was finally obtained by a crystallization from CH_3CN, in which only extremely thin needles were present. An orthorhombic cell of space group *Amma* (nonstandard setting of *Cmcm*) was characterized with cell dimensions at −162 °C of a = 12.414 (12), b = 7.683 (7), and c = 14.583 (15) Å. The cell volume of 1390.8 (6) Å^3 gives a density of 2.217 g cm^{-3} for Z = 4, indicating the molecule must possess *mm* or $2/m$ symmetry. A total of 790 reflections were collected in the range $5° \leq 2\theta \leq 45°$ and reduced to 517 unique intensities. A scan speed of 2.0° min^{-1} and 10-s stationary background counts were used because of the low scattering of the crystal. The data were corrected for absorption (μ = 105.7 cm^{-1}), and the minimum and maximum transmission coefficients were 0.253 and 0.811, respectively.

The structure was solved by direct methods and Fourier techniques and possesses *mm* crystallographic symmetry. Full-matrix refinement using anisotropic thermal parameters converged to $R(F)$ = 0.078 and $R_w(F)$ = 0.065. A difference Fourier synthesis indicated several peaks of density 4.0–5.0 e Å^{-3} near the platinum, and the random distribution of numerous peaks of density 0.6–1.0 e Å^{-3} precluded the unequivocal assignment of hydrogen atoms. The refinement was concluded when the maximum shift/error was less than 0.10 and the goodness of fit for the first cycle was 2.105.

(bpy)Pt(COCH$_2$CH$_2$CH$_3$)$_2$. A suitable crystal was obtained by cleaving the bright red needles to obtain an irregularly shaped crystal of 0.06-mm maximum dimension. The selected crystal was thermochromic, changing from red to orange as it was cooled to −168 °C. The space group was determined to be $P2_1/a$ (nonstandard setting of $P2_1/c$) with cell dimensions at −168 °C of a = 16.195 (7) Å, b = 14.775 (6) Å, c = 7.085 (2) Å, and β = 93.31 (2)°. The density is calculated as 1.937 g cm^{-3} assuming Z = 4 for a volume of 1692.5 (1) Å^3. Data collection parameters were identical with those of (bpy)PtC$_3$H$_6$ presented above. A total of 2611 intensities were collected for $5° \leq 2\theta \leq 50°$ and reduced to 2229 unique data, of which 1649 had $F_o \geq 2.33\sigma(F_o)$. Manual ψ scans and an examination of symmetry-related intensity indicated a maximum absorption of ca. 10%. Due to the irregular shape of the sample, no attempt was made to perform this correction.

The structure was solved by a combination of Patterson and Fourier techniques. A difference Fourier synthesis phased on the refined non-hydrogen parameters located all but two hydrogen atoms. Attempts to include hydrogen parameters in the refinement were unsuccessful, since several refused to converge. In the final cycles of full-matrix refinement, hydrogen contributions were included as fixed atom contributors with d(C–H) = 0.95 Å, and all angles fixed as sp_3 or sp_2 coordination. Final residuals were $R(F)$ = 0.057 and $R_w(F)$ = 0.054, and the goodness of fit for the last cycle was 1.293. The maximum shift/error for the final cycle was 0.05.

Acknowledgment. We wish to thank K. L. Rollick for help with the temperature-dependent ^{1}H NMR spectra, K. S. Chen for carrying out some of the ESR experiments, Johnson Matthey, Inc., for a generous loan of platinum, and the National Science Foundation for financial support.

Registry No. I, 78179-73-4; IIa, 80925-63-9; IIb, 80925-64-0; IIc, 80925-65-1; IId, 80925-66-2; III, 80925-67-3; IV, 80925-68-4; V, 80939-24-8; $Cl_2(bpy)PtC_3H_6$, 23128-96-3; CO, 630-08-0; SO_2, 7446-09-5; $(Ph_3P)_2Pt(CH_2CH_3)_2$, 43097-18-3; $(bpy)PtCl_2$, 13965-31-6.

Supplementary Material Available: Complete listing of anisotropic thermal parameters (Table X), observed and calculated structure factors (Table XI), hydrogen bond distances and angles (Table XII), and hydrogen fractional coordinates and isotropic thermal parameters (Table XIII) (36 pages). Ordering information is given on any current masthead page.

Synthesis and Reactivity of New Polyhydride Compounds of Tantalum(V)

James M. Mayer[1] and John E. Bercaw*[2]

Contribution No. 6519 from the Arthur Amos Noyes Laboratory of Chemical Physics, California Institute of Technology, Pasadena, California 91125. *Received August 20, 1981*

Abstract: A series of (pentamethylcyclopentadienyl)tantalum bis(phosphine) polyhydride complexes, $(\eta^5\text{-}C_5Me_5)TaL_2H_{4-n}Cl_n$ (n = 0, L = PMe_3, $PMe_2(C_6H_5)$, $P(OMe)_3$, and $Me_2PCH_2CH_2PMe_2$; n = 1, L = PMe_3), have been prepared by high-pressure hydrogenation of $(\eta^5\text{-}C_5Me_5)TaMe_4$ or $(\eta^5\text{-}C_5Me_5)TaMe_3Cl$ in the presence of L. The hydride ligands are more hydridic than protic in character. All of the compounds react with acetone and methanol to afford isopropoxide and methoxide complexes, respectively. Reactions with carbon monoxide yield carbonyl hydride and dicarbonyl compounds resulting from sequential reductive elimination of dihydrogen. Hydrogenation of ethylene is observed as well as catalytic dimerization of ethylene to 1-butene. Most reactions of these 18-electron polyhydride complexes are thought to involve rate-determining loss of a phosphine ligand. Evidence is presented in support of coordination of acetone to tantalum prior to its reduction to isopropoxide. By contrast, methanol can react directly with the coordinatively saturated tantalum hydride species to generate H_2.

Polyhydride complexes have been isolated for most of the transition metals, often with phosphines as the only other ligands.[3] The primary focus of this research has been the definition of the solid-state structures and the fluxional processes that are very common for these molecules.[3,4] Polyhydride compounds have high coordination numbers (6–9) and are among the least sterically crowded examples of these coordination geometries. The formal oxidation states for the metal center in early and middle transition-metal polyhydrides are often high, with d^2 and d^0 configurations quite common. The chemistry of transition-metal polyhydride complexes, especially those with formal d^0 configurations, has not yet been systematically examined. This may be due to the fact that these compounds are nearly always coordinatively saturated and thus relatively inert.[5] Lower valent "hydrides" are generally chemically more protic than hydridic: they are stable to alcohols, can often be deprotonated with strong bases, and can usually be protonated by strong acids without loss of dihydrogen.

Our interest in d^0 transition-metal hydride complexes was stimulated by the wealth of chemistry we found for bis(pentamethylcyclopentadienyl)zirconium dihydride, $Cp^*_2ZrH_2$ (**1**) ($Cp^* = \eta^5\text{-}C_5(CH_3)_5$).[6] **1** is unusual both because its zirconium–hydride

(1) National Science Foundation Predoctoral Fellow, 1978–1981.
(2) Camille and Henry Dreyfus Teacher-Scholar, 1977–1982.
(3) (a) *Adv. Chem. Ser.* **1978**, *No.* 167. (b) "Transition Metal Hydrides"; Muetterties, E. L., Ed.; Marcel Dekker: New York, 1971. (c) Kaesz, H. D.; Saillant, R. B. *Chem. Rev.* **1972**, *72*, 231.
(4) Meakin, P.; Guggenberger, L. J.; Peet, W. G.; Muetterties, E. L.; Jesson, J. P. *J. Am. Chem. Soc.* **1973**, *95*, 1467–1474.
(5) Collman, J. P.; Hegedus, L. S. "Principles and Applications of Organotransition Metal Chemistry"; University Science Books: Mill Valley, CA, 1980; p 62.

0002-7863/82/1504-2157$01.25/0